

R. J. Stern · M. G. Abdelsalam

Formation of juvenile continental crust in the Arabian–Nubian shield: evidence from granitic rocks of the Nakasib suture, NE Sudan

Received: 16 January 1997 / Accepted: 30 November 1997

Abstract Major and trace element data, U–Pb zircon ages, and initial isotopic compositions of Sr, Nd, and Pb are reported for ten granitic and one rhyolitic rock sample from the neo-Proterozoic Nakasib suture in NE Sudan. Chemical data indicate that the samples are medium- to high-K, “I-type” granitic rocks that mostly plot as “volcanic arc granites” on discriminant diagrams. Geochronologic data indicate that rifting occurred 790 ± 2 Ma and constrain the time of deformation associated with suturing of the Gebeit and Haya terranes to have ended by approximately 740 Ma. Isotopic data show a limited range, with initial $^{87}\text{Sr}/^{86}\text{Sr} = 0.7021$ to 0.7032 (mean = 0.7025), $\epsilon\text{Nd}(t) = +5.5$ to $+7.0$ (mean = $+6.4$), and $^{206}\text{Pb}/^{204}\text{Pb} = 17.50$ – 17.62 . Neodymium model ages (T_{DM} ; 0.69 – 0.85 Ga; mean = 0.76 Ga) are indistinguishable from crystallization ages (0.79 – 0.71 Ga; mean = 0.76 Ga), and the isotopic data considered together indicate derivation from homogeneously depleted mantle. The geochronologic data indicate that the terrane accretion to form the Arabian–Nubian shield began just prior to 750 Ma. The isotopic data reinforces models for the generation of large volumes of juvenile continental crust during neo-Proterozoic time, probably at intra-oceanic convergent margins. The data also indicate that crust formation was associated with two cycles of incompatible element enrichment in granitic rocks, with an earlier cycle beginning approximately 870 Ma and culminating approximately 740 Ma, and the second cycle beginning after pervasive high-degree melts – possibly hot-spot related – were emplaced approximately 690–720 Ma.

Key words Arabian-Nubian shield · Continental crust · granites · Sra isotopes · Nd-isotopes · Pb-isotopes · U-Pb zircon ages

Introduction

The Arabian–Nubian shield (ANS) is a superb example of the formation of juvenile continental crust formation during neo-Proterozoic time (Pallister et al. 1988; Stern and Kröner 1993). The ANS crust comprises several terranes sutured together approximately 700–800 Ma ago (Stoeser and Camp 1985; Vail 1985). It is important to understand ANS crustal evolution for several reasons including:

1. It contains abundant evidence of ophiolites and therefore is the most convincing demonstration that sea-floor spreading occurred in Precambrian times.
2. It is one of the few places on earth where the formation of a vast tract of continental crust can be clearly related to plate tectonic processes (Dixon and Golombek 1988; Reymer and Schubert 1984).
3. The concentration of neo-Proterozoic juvenile crust in the region constrains models for the assembly of continental crust and evolution of oceanic Sr, C, and S reservoirs during this important time in earth history (Stern 1994).

Neo-Proterozoic crustal evolution in the ANS continues to attract attention. In addition to the existing arc accretion paradigm (Vail 1985; Stoeser and Camp 1985), two new models have recently been proposed: the hot spot model of Stein and Goldstein (1996), whereby most of the ANS crust is due to accretion of oceanic plateaux, and the Turkic-type orogenic model of Sengör and Natal'in (1996) whereby much of the ANS crust formed in broad forearc complexes. Refinement and testing of these models require chemical, chronologic, and isotopic data for vast expanses of particularly NE Africa, but comprehensive chemical and isotopic data sets for well-dated plutonic suites are scarce. We report here chemical, geochronological, and isotopic data for a suite of granitic intrusions from the Nakasib suture in NE Sudan. These data indicate that the interval 790–710 Ma was an important period of juvenile crust formation in NE Sudan, and that two enrichment cycles may be distinguished for ANS granitic rocks.

Regional setting and previous work

Following its recognition a little over a decade ago (Embleton et al. 1984) the Nakasib suture has become the focus of detailed studies for two reasons:

1. This is one of the best places in the ANS to examine processes of terrane formation and accretion, because the suture zone preserves a distinctive stratigraphic succession and deformation history.
2. The western part of the Nakasib suture – locally known as the Ariab belt – contains important stratabound gold deposits (Wipfler 1994), as does the eastern continuation of the suture in Arabia (Nassief et al. 1984; Johnson 1994). The Nakasib suture (sometimes referred to as the “Ariab-Nakasib Belt”; Wipfler 1994) separates the 660–830 Ma Gebeit terrane to the north from the 820–890 Ma Haya terrane to the south (Kröner et al. 1991; Reischmann et al. 1992; Stern and Kröner 1993; Reischmann and Kröner 1994). Despite the fact that it is the oldest known suture in the ANS, the Nakasib suture is in many ways the most unequivocal and best preserved of all (Stern and Kröner 1993; Abdelsalam and Stern 1993a).

The Nakasib suture is extrapolated across the Red Sea into Saudi Arabia through ophiolitic units at Jebel Thurwah to those at Bir Umq. Closing the Red Sea, the entire Ariab-Nakasib-Bir Umq suture can be traced for approximately 700 km between its truncation to the east by the Nabitah suture in Arabia and to the west by the Keraf suture in Sudan (Abdelsalam and Stern 1996a, b). Differing preservation states of the suture and approaches of geologic studies in Arabia and Sudan provide different perspectives. The supracrustal section and sequence of nappes is better resolved in Sudan, whereas the ophiolite itself is better known from studies in Arabia. U–Pb zircon and Sm–Nd ages for Bir Umq ophiolitic rocks are approximately 830 Ma (Dunlop et al. 1986; Pallister et al. 1988), whereas a zircon fraction from the Thurwah ophiolite yielded an age of 870 Ma (Pallister et al. 1988). The same sample yielded xenocrystic zircons with $^{207}\text{Pb}/^{206}\text{Pb}$ model ages of approximately 1250 Ma, which calls into question interpretation of the 870 Ma date as a magmatic age.

Detailed studies in the SW part of the suture have been carried out by scientists from the Technical University in Berlin (Bakheit 1991; Abdel Rahman 1993; Schandelmeier et al. 1994; Wipfler 1994, 1996) and by us in the NE part of the suture (Abdelsalam and Stern 1993a, b; Abdelsalam 1993, 1994). The two groups disagree on two important points. Firstly, we infer a complete Wilson cycle, progressing from rifting to sea-floor spreading and subduction, culminating in collision between the Gebeit terrane to the north and the Haya terrane to the south (Abdelsalam and Stern 1993b), whereas the Berlin group sees no evidence for the early rifting phase (Schandelmeier et al. 1994). We interpret the stratigraphic succession (Arbaat volcanics, Meritri sediments, and Salatib sediments of Abdelsalam and Stern 1993a) as reflecting the development of a passive margin, whereas the Berlin group interprets

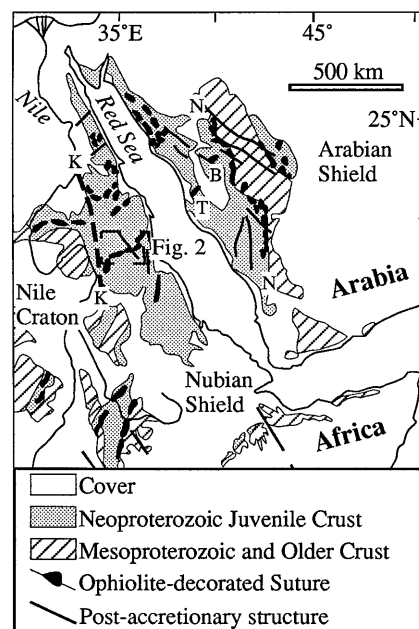


Fig. 1 Generalized geologic map of the Arabian–Nubian shield, showing the location of the Nakasib suture (inside dashed box, labeled Fig. 2) and related tectonic elements, as discussed in text. Dashed line K–K is Keraf suture. Continuation of the Nakasib suture in Arabia as the Bir Umq suture is also shown. T Thurwah ophiolite; B Bir Umq ophiolite. (Modified after Worku and Schandelmeier 1996)

the supracrustal succession as an arc–forearc sequence. Secondly, we infer a north-dipping subduction zone that led to collision and emplacement of southward-directed ophiolitic and supracrustal nappes, whereas the Berlin group infer that south-dipping subduction led to collision and emplacement of northward-directed ophiolitic nappes. We interpret the two NE-trending parallel ophiolite belts as being the eroded limbs of a NE-trending antiform, whereas the Berlin group interprets these as separate, chemically distinct ophiolite belts. It is noteworthy that the Thurwah ophiolite was thrust southwards (Johnson 1994) and that the Bir Umq ophiolite was thrust from north to south over Mahd group sediments (Pallister et al. 1988).

Studies of the granitic rocks of the Nakasib suture can help resolve these controversies by providing insights into the crust-forming process as well as constraining deformation timing. A few of these plutons have been studied for chemical compositions and Rb/Sr and zircon evaporation geochronology (Almond et al. 1989; Schandelmeier et al. 1994). We expand on this database and present here chemical, isotopic, and geochronologic data for several plutons from along the suture zone along with a single rhyolite from the Arba’at volcanics. Most samples were collected in the course of structural and stratigraphic field studies of the eastern and central portions of the suture, reported by Abdelsalam and Stern (1993a, b) and Abdelsalam (1994). We also report initial Sr and Nd isotopic data for three granitic samples from the western part of the suture previously studied by Schandelmeier et al. (1994). All except 48–1 are samples of intermediate to felsic plutons; 48–1 is a

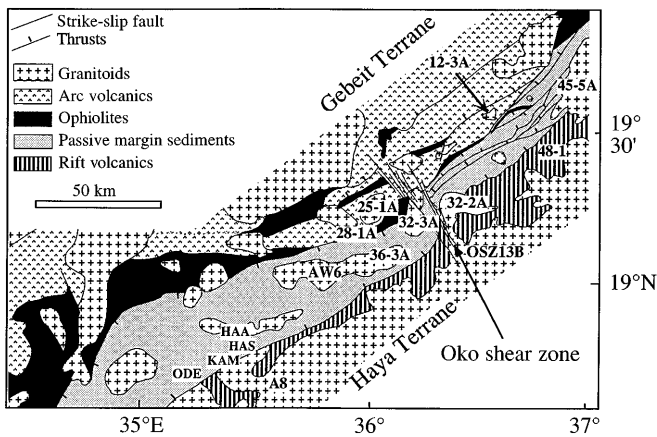


Fig. 2 Generalized geologic map of the Nakasib suture showing sample localities, modified after Johnson (1994). Gold deposits of the Ariab district are labeled *HAA* (Hadal Auatib), *HAS* (Hassai), *KAM* (Kamoeb), and *ODE* (Oderuk)

rhyolite associated with the early stages of rifting (Abdelsalam and Stern 1993b). Samples A8, OSZ13, and AW6 are from the study of Schandemeier et al. (1994), who identified four distinct granitoid associations: (a) gabbro–diorite–tonalite; (b) granodiorite–trondhjemite; (c) granite; and (d) syenite. A8 (Adaiamet diorite) is from the gabbro–diorite–tonalite association and yields a zircon evaporation age of 810 ± 12 Ma, OSZ13 (Jebel Tala granodiorite) is 812 ± 18 Ma and is part of the granodiorite–trondhjemite association, and AW6 (Wadi Agwampt granite) is from the granite association and is 762 ± 23 Ma. We interpret the locations of the Adaiamet diorite and Jebel Tala granodiorite to lie south of the zone affected by Nakasib deformation, so that these plutons are intruded into the northern margin of the Haya terrane. If this interpretation is correct, then the >800 -Ma ages obtained for these samples do not constrain the timing of deformation in the Nakasib suture. The samples analyzed for this study are representative of all but the syenitic suite, which is a minor and much younger (523 ± 18 Ma; Schandemeier et al. 1994) plutonic suite in the region.

According to our structural studies (Abdelsalam and Stern 1993a, b; Abdelsalam 1994), the Nakasib suture evolved through three deformation phases (D_1 , D_2 , and D_3) associated with docking of the Haya and Gebeit terranes. D_1 and D_2 are NW-verging folds and thrusts, whereas D_3 refolded D_1 and D_2 into NW-trending, upright folds. Deformation associated with the Oko shear zone was superimposed on the earlier structures in the form of early, north-trending upright folds (D_4) and late NW-trending, sinistral strike-slip faults (D_5). Below is a brief description of the spatial and temporal setting of the samples used for this study, listed from east to west and plotted in Fig. 2.

1. Arbaat Pluton (45–5A): This lies in the NE part of the Nakasib suture. The sample studied here was collected along Khor Arbaat. It is a quartz diorite, predominantly composed of plagioclase and green amphibole, with some interstitial quartz. Local NE-trending foliation in-

dicates that the pluton experienced at least part of the deformational history of the Nakasib suture.

2. Arbaat volcanics (48–1): This is from the same locality as H13-7 of Abdelsalam and Stern (1993b). The Arbaat volcanics are dominant tholeiitic basalts and subordinate felsic lavas interpreted as erupted during rifting.
3. Meritri Pluton (12–3A): This is a small (~ 5 km diameter) pluton in the NE part of the Nakasib suture. It is exposed along the northern part of Khor Meritri. It is a biotite granite composed of subequal proportions of quartz and K-feldspar and subordinate plagioclase and biotite. The pluton is free of planar or linear fabrics and is interpreted as a post-tectonic intrusion.
4. Tendily Pluton (32–2A): This is a 20-km-long, 12-km-wide body which lies just east of the Oko shear zone. It is a medium-grained, pink, biotite granite made up of quartz, K-feldspar, plagioclase, and biotite. The pluton lacks a deformational fabric and is mapped as a post-tectonic intrusion.
5. Hantouly Pluton (32–3A): This body is a 20-km-long, 10-km-wide intrusion which lies within the Nakasib suture along the western side of the Oko shear zone. It is a biotite granite composed of K-feldspar, quartz, plagioclase, and biotite. Deformation fabrics related to the Nakasib suture cannot be identified, but the pluton is cut by one strand of the Oko shear zone and contains a NNW-trending fabric related to Oko deformation.
6. Shalhout Pluton (25–1A): This body occupies the core of an antiform in the Nakasib suture SW of the Oko shear zone. It occurs as a circular body approximately 15 km in diameter. It is a heterogeneous body ranging from hornblende diorite to adamellite. The sample analyzed here is adamellite, with subequal proportions of plagioclase and K-feldspar and subordinate quartz and biotite. The pluton is interpreted to be a syntectonic intrusion, with fabrics suggesting emplacement before D_3 but after D_2 . This pluton was also studied by Almond et al. (1989) who reported a Rb/Sr whole-rock isochron age of 697 ± 5 Ma.
7. Unnamed Pluton (28–1A): The sample is from a small granitic body (not mappable at scale of 1:70000) which lies close to the Igariri ophiolite, but intrudes the volcano-sedimentary sequence to the north of the ophiolite complex. The granite is one of a series of E–W elongated small bodies which are deformed with the D_1/D_2 foliation. The sample was collected because it is a muscovite granodiorite, possibly indicating melting of older sediments. It is composed of muscovite, biotite, quartz, plagioclase, and K-feldspar.
8. Luggag Pluton (36–3A): This occupies the core of a broad synform along the SW part of the Nakasib suture. The pluton is circular and approximately 10 km across. It is heterogeneous, with dominant adamellite and minor granite, composed of differing proportions of K-feldspar, quartz, biotite, and plagioclase. This pluton is interpreted to be a syntectonic intrusion, with fabrics suggesting emplacement before D_3 but after D_2 .

Table 1 Major and trace element compositions

	OSZ 13b ^b	A8 ^b	45-5A	H13-7 ^c	AW-6 ^b	25-1A	12-3A	32-2A	36-3A	32-3A	28-1A
SiO ₂	70.9	65.8	63.1	75.3	75.7	68.5	74.9	75.8	67.0	72.2	72.9
TiO ₂	0.63	0.49	0.80	0.28	0.18	0.53	0.18	0.21	0.75	0.41	0.17
Al ₂ O ₃	13.7	15.7	16.2	13.4	12.7	16.2	13.5	13.0	15.4	14.1	15.1
Fe ₂ O ₃	3.70	5.08	7.05	1.87	1.77	3.62	1.83	1.55	4.84	3.23	2.16
MgO	0.85	2.40	2.13	0.20	0.17	1.19	0.36	0.23	1.25	0.73	0.43
CaO	3.05	5.37	5.35	1.49	0.97	3.55	1.34	0.82	3.20	2.15	1.62
Na ₂ O	4.11	3.48	4.46	5.04	3.53	4.47	4.17	4.33	4.15	3.98	4.05
K ₂ O	2.94	1.59	0.60	2.38	4.94	1.84	3.68	4.05	3.20	3.06	3.49
P ₂ O ₅	0.14	0.12	0.29	0.07	0.06	0.13	0.04	0.02	0.22	0.12	0.08
Rb ^a	58.3	23.4	8.29	18.9	68.3	57.3	85.4	98.7	64.6	36.7	–
Sr ^a	192	442	362	363	61.1	388	93.8	64.2	277	163	–
Zr	315	108	113	344	186	240	124	170	343	173	–
Nb	5	2	1.9	10.4	7	4.3	10	7.1	19.8	6	–
Y	38	19	28	51	34	15	52	35	43	23	–
Nd ^a	30.8	14.0	20.8	35.8	31.2	12.3	22.5	30.6	38.4	31.2	18.0
Sm ^a	6.40	3.05	5.12	7.72	6.59	2.70	5.41	5.96	8.08	6.00	3.78
K/Rb	419	564	600	1045	600	267	358	342	411	692	–
Sr/Y	5.1	23	13	7.1	1.8	26	1.8	1.8	6.4	7.1	–

NOTE: Major element totals normalized to 100% anhydrous

^a Data by isotope dilution (this study)^b Data from Schandelmeier et al. (1994)^c Data from Abdelsalam and Stern (1993)

Analytical techniques

Samples for whole-rock analyses, including major and trace element analyses and Sm–Nd and Rb–Sr analyses, were pulverized in agate. Major elements and Zr, Y, and Nb were determined by XRF at the University of Oklahoma using techniques outlined by Weaver (1990). Rb, Sr, Sm, and Nd concentrations in whole-rock powders were determined by isotope dilution at UTD, following dissolution in Krogh-type bombs and other procedures outlined in Stern and Kröner (1993). Techniques for the analysis of Sr and Nd isotopic compositions of whole-rock powders, U–Pb zircon age determinations, and Pb isotopic compositions of feldspars are also presented in Stern and Kröner (1993). Pb isotopic analyses were corrected for fractionation @0.15%/AMU. Eight analyses of NBS-981 yielded

$^{206}\text{Pb}/^{204}\text{Pb}=16.944\pm 5$; $^{207}\text{Pb}/^{204}\text{Pb}=15.500\pm 6$; $^{208}\text{Pb}/^{204}\text{Pb}=36.743\pm 18$ (total range). Data is adjusted to a value for E&A SrCO₃ $^{87}\text{Sr}/^{86}\text{Sr}=0.70800$. Accuracy on $^{87}\text{Sr}/^{86}\text{Sr}$ for these is better than ± 0.00004 . Multiple analyses of Nd standards yielded mean $^{143}\text{Nd}/^{144}\text{Nd}$ of 0.511838 and 0.512613 for the UCSD and BCR-1 standards, respectively. Calculation of initial Nd [$\epsilon\text{Nd}(t)$] and Sr isotopic compositions is based on Sm/Nd and Rb/Sr from Table 1. Nd model ages are calculated after the algorithm of Nelson and DePaolo (1985). Crystallization ages are taken from U–Pb zircon data of Table 1, evaporation ages of Schandelmeier et al. (1994), or from the Rb–Sr age of 696 Ma (Almond et al. 1989) for 25–1A. A minimum age of 710 Ma is assumed for sample 28–1A for calculation of $\epsilon\text{Nd}(t)$.

Table 2 U–Pb zircon data

Sample, mesh	U (ppm)	Pb (ppm)	$^{204}\text{Pb}/^{206}\text{Pb}$	$^{207}\text{Pb}/^{206}\text{Pb}$	$^{207}\text{Pb}^*/^{206}\text{Pb}^*$	$^{207}\text{Pb}^*/^{235}\text{U}$	$^{206}\text{Pb}^*/^{238}\text{U}$	% Discordance	Age (Ma)
48-1									
+270	156.7	25.4	0.003845	0.12088	0.06551 ^a	1.207	0.1337	– 2.4	790±2
–270 +325	189.3	29.3	0.003044	0.10851	0.06544 ^a	1.167	0.1294	0.8	
45-5									
+100	244.3	33.4	0.001389	0.08517	0.06516 ^a	1.102	0.1226	4.2	779±3
12-3A									
–230	1057	125	0.000889	0.07701	0.06419 ^b	0.9770	0.1104	9.8	748±3
32-2A									
–200 +270	1152	97.0	0.000730	0.07490	0.06437 ^b	0.6763	0.0762	37	754±3
32-3A									
–200	759	84.3	0.000204	0.06606	0.06310 ^b	0.8935	0.1028	11	710±3
36-3A									
–100 +140	641	55.5	0.000641	0.07322	0.06396 ^b	0.7467	0.0847	15	740±3

^a Corrected for common Pb at 800 Ma (Stacey and Kramers 1975)^b Corrected for common Pb at 750 Ma (Stacey and Kramers 1975)

Table 3 Sr and Nd isotopic data

Sample	$^{87}\text{Rb}/^{86}\text{Sr}$	$^{87}\text{Sr}/^{86}\text{Sr}$	$^{87}\text{Sr}/^{86}\text{Sr}_i$	$^{147}\text{Sm}/^{144}\text{Nd}$	$^{143}\text{Nd}/^{144}\text{Nd}_0$	$\epsilon\text{-Nd(T)}^c$	T_{DM} (Ga)
45-5	0.0663	0.70322	0.7025	0.149	0.51273	+7.0	0.71
48-1 ^a	0.151	0.70403	0.7023	0.130	0.51262	+6.8	0.75
12-3A	2.64	0.73039	0.7022	0.146	0.51265	+5.5	0.85
32-2A	4.42	0.74752	n.r.	0.118	0.51255	+6.3	0.76
32-3A	0.653	0.70974	0.7031	0.116	0.51257	+6.4	0.72
25-1A ^b	0.427	0.70711	0.7029	0.133	0.51262	+5.7	0.77
28-1A	—	—	—	0.127	0.51262	+6.3 ^d	0.72
36-3A	0.675	0.70926	0.7021	0.127	0.51264	+7.0	0.69
A8	0.153	0.70453	0.7028	0.132	0.51257	+5.8	0.85
AW6	3.243	0.73617	n.r.	0.128	0.51262	+6.8	0.73
OSZ-13b	0.878	0.71225	0.7021	0.126	0.51259	+6.8	0.76

^a Actual samples are H17-2 (Rb-Sr) and H13-7 (Sm-Nd), collected from same locality as 48-1

^b Rb-Sr whole-rock age of 696 Ma from Almond et al. (1989)

^c t = U-Pb zircon age, evaporation age from Schandelmeier et al. (1994), or Rb-Sr whole-rock age from Almond et al. (1989)

^d t = 700 Ma (assumed)

Table 4 K-feldspar Pb isotopic compositions

Sample	$^{206}\text{Pb}/^{204}\text{Pb}$	$^{207}\text{Pb}/^{204}\text{Pb}$	$^{208}\text{Pb}/^{204}\text{Pb}$
12-3A	17.624	15.480	37.115
32-3A	17.620	15.510	37.149
36-3A	17.503	15.448	36.948
45-5	17.552	15.460	37.001

Results

Major and trace element data are reported in Table 1, U–Pb zircon data and ages are reported in Table 2, Sr- and Nd isotopic data are reported in Table 3, and Pb isotopic compositions of feldspars are listed in Table 4. U–Pb ages for six samples listed in Table 2 range between 710 and 790 Ma. The data define a period of approximately 40 million years for the evolution of the Nakasib suture, from rifting at 790 Ma to the end of D_1/D_2 deformation by the time of intrusion of the Tendily and Meritri plutons at 754 and 748 Ma, respectively, although the late tectonic nature of the 740-Ma Luggag pluton suggests that deformation may have continued after this time in the west. Minor igneous activity continued until 710–696 Ma. The age data presented here along with the studies of Almond et al. (1989) and Schandelmeier et al. (1994) provide nine samples dated with U–Pb zircon techniques and one by Rb–Sr whole-rock techniques, permitting examination of chemical and isotopic compositions within a temporal framework. Note that because 28–1A has not been dated, it is not used in following discussions except regarding its Nd isotopic composition. Because there is evidence for a ca. 700-Ma thermal resetting episode in the region (Abdelsalam 1993), the Rb–Sr age of 696 Ma for 25–1A should be regarded as a minimum.

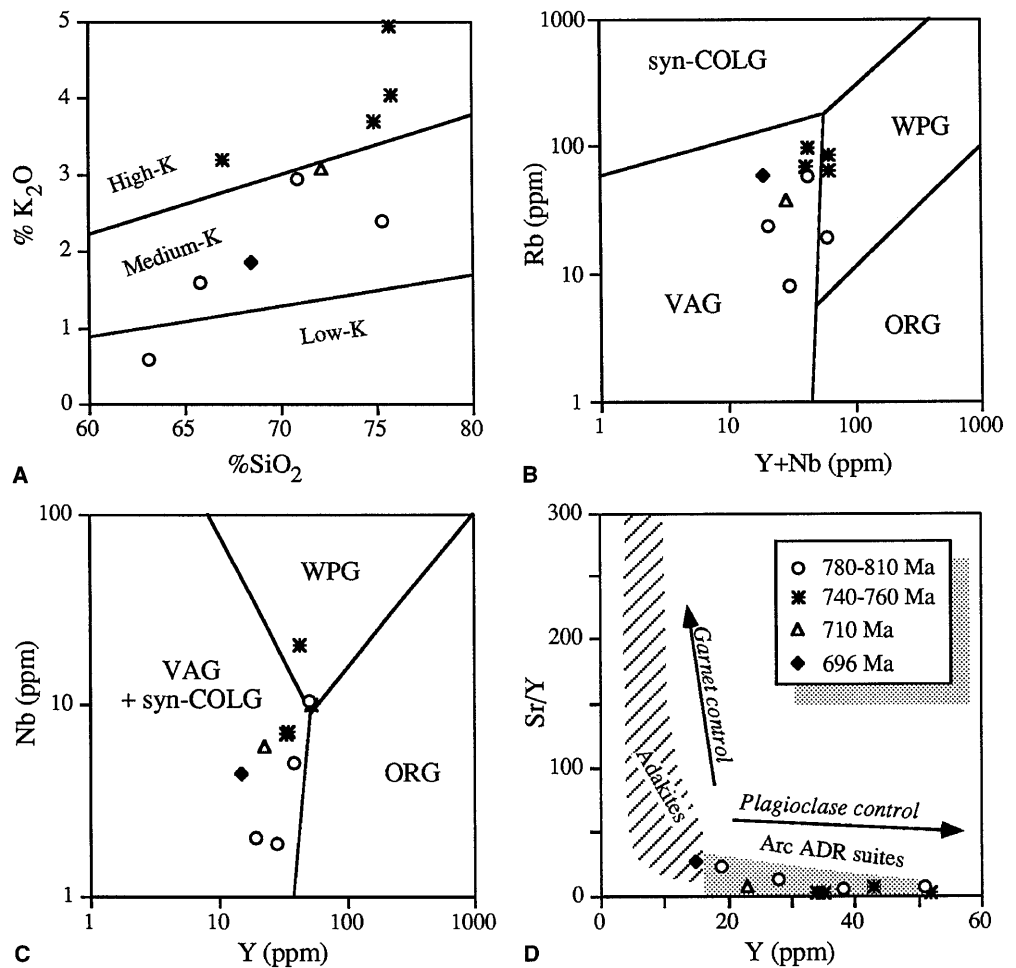
Chemical data indicate that the samples mostly plot in the field of medium- to high-K felsic rocks (Fig. 3a), with the older rocks (779–812 Ma) generally being less potassic

and more mafic than the 740–762 Ma granitic rocks. The two youngest samples (696–710 Ma) do not continue this trend but return to the medium-K field. With the possible exception of 28–1A, which may be an S-type granitoid, other plutonic rocks are I-type granitoids. Although the data mostly plot in the fields of “volcanic arc granite” on felsic rock discriminant diagrams (Fig. 3b,c), these data also suggest an interrupted progression of enrichment, from 812- to 779-Ma plutons with lower Rb, Y, and Nb succeeded by more enriched 740- to 762-Ma plutons, followed by a return to lower Rb, Y, and Nb in the youngest plutons.

The petrogenesis of Nakasib plutonic rocks is beyond the scope of this study, but a few comments are appropriate. Figure 3d summarizes two fundamentally different groups of felsic igneous rocks, Adakites and ADR suites, which reflect relatively high- and low-pressure melt equilibrium, respectively. Adakites have trace element characteristics that indicate equilibrium with garnet (high Sr/Y and low Y contents; steep rare earth element patterns that commonly lack an Eu anomaly). Such conditions exist for melting of eclogitic subducted crust or garnet granulite lower continental crust. Felsic igneous rocks with adakite characteristics are found among Archean granitic rocks (Martin 1986) and modern slab melts (Drummond and Defant 1990). Melting of the subducted slab presently occurs only where very young and therefore hot crust is subducted, but may have been more common earlier in earth history. Compositional features characteristic of adakites have been reported for approximately 25% of 860- to 820-Ma granitoids of the Arabian shield (Harris et al. 1993).

In contrast, felsic igneous rocks with low Sr/Y and high Y contents define the Arc ADR (andesite–dacite–rhyolite) suites field. These compositional features (along with rare earth element patterns with a negative Eu anomaly) signify magmatic equilibrium with plagioclase (\pm amphibole, pyroxene). This can occur either during melting of amphibolite-facies crust or low-pressure melt fractionation, as has been discussed by Beard (1995). All of the Nakasib granitic rocks studied here and by Schandelmeier et al. (1994) plot in the ADR field, indicating modes of generation like

Fig. 3A–D Geochemical characteristics of Nakasib granitic rocks. **A** K_2O – SiO_2 diagram, after Ewart (1979); **B** Tectonic discriminant diagram Rb vs Nb+Y (Pearce et al. 1984); **C** Tectonic discriminant diagram Nb vs Y (Pearce et al. 1984); **D** Petrogenetic diagrams for adakites vs arc andesite–dacite–rhyolite (ADR) suites (Drummond and Defant 1990), showing control by garnet to form adakitic felsic melts and plagioclase to form the ADR suite



those of modern ADR suites. The Nakasib granitic rocks formed by magmatic processes that cannot be distinguished from those of modern convergent margins, an observation that is also consistent with where the Nakasib data plot on discriminant diagrams (Fig. 3b, c).

Initial $^{87}Sr/^{86}Sr$ are reported for eight samples in Table 3, and these data are plotted in Fig. 4. Note that initial $^{87}Sr/^{86}Sr$ is not calculated for two samples with $^{87}Rb/^{86}Sr > 3$. The remaining eight samples have initial $^{87}Sr/^{86}Sr$ ranging between 0.7021 and 0.7032, with a mean of 0.7025. These initial ratios are indistinguishable from initial ratios reported from juvenile crust in the Arabian shield to the north and 700 ± 150 -Ma lithospheric mantle from beneath the Arabian shield (Henjes-Kunst et al. 1990; Stern and Kröner 1993; Stern and Hedge 1985). These ratios are only slightly more radiogenic than the composition expected for a depleted MORB-type mantle of neo-Proterozoic age (Stern and Hedge 1985). The initial $^{87}Sr/^{86}Sr$ indicate little or no crustal residence time for Nakasib felsic rocks, i.e., they were formed either directly by fractionation of mantle-derived melts or indirectly, by melting of mantle-derived rocks.

Initial Nd data are reported in Table 3 as $\epsilon(t)$, where t refers to the crystallization age, or as T_{DM} , which is a model age calculated from the intersection of the sample's ra-

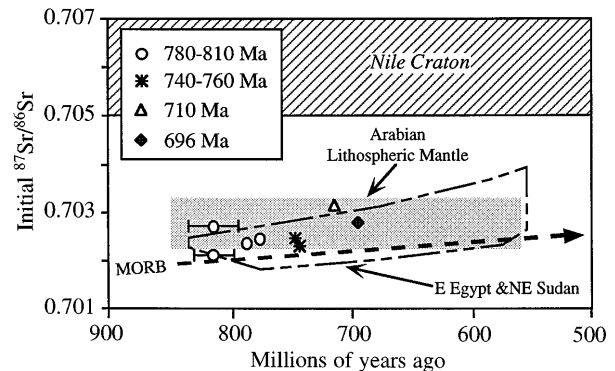


Fig. 4 Initial $^{87}Sr/^{86}Sr$ vs age of Nakasib granitic rocks. These data are similar to fields defined by igneous rocks farther north in Sudan (field labeled *E Egypt & NE Sudan*; Stern and Kröner 1993; Stern and Hedge 1985). Field labeled *Arabian Lithospheric Mantle* shows the initial $^{87}Sr/^{86}Sr$ for xenoliths sampling the subcontinental lithospheric mantle beneath Arabia, from the results of Henjes-Kunst et al. (1990). Field labeled *Nile Craton* generalizes the lower limit of initial $^{87}Sr/^{86}Sr$ for basement west of the Nile (Stern and Kröner 1993). The inferred trajectory of MORB-type depleted mantle is shown with a dashed line, after Stern and Hedge (1985)

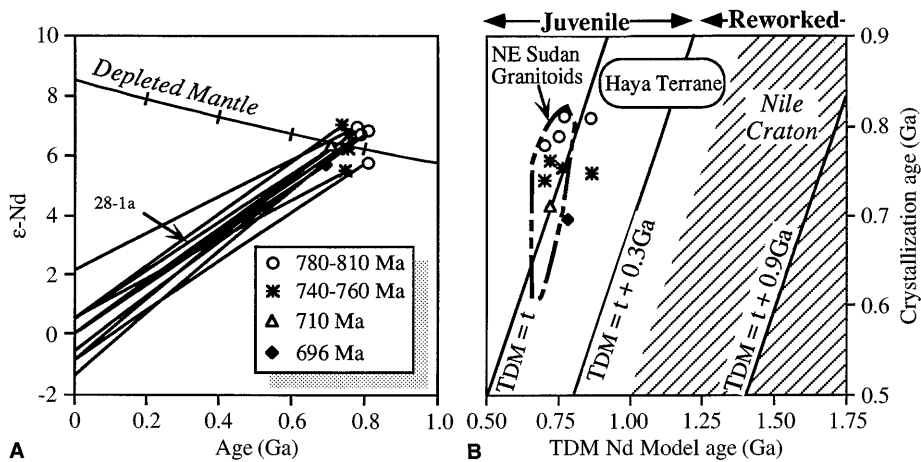
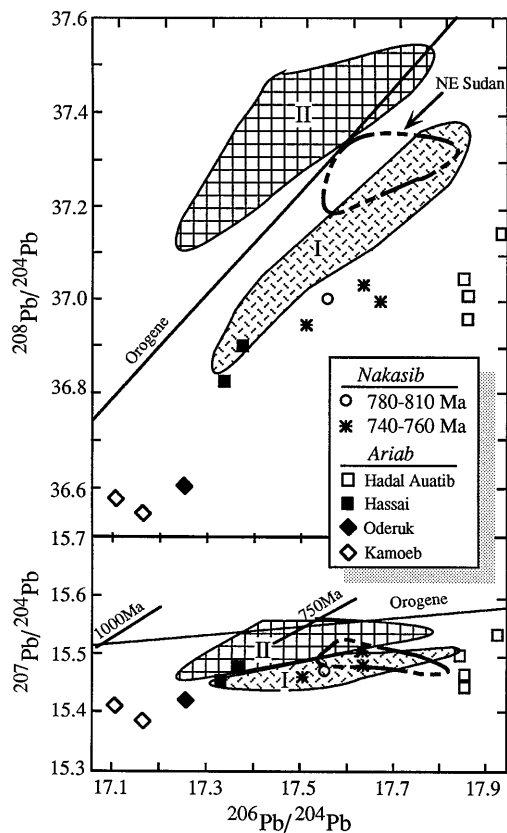


Fig. 5 Nd isotopic systematics for **A** Nakasib felsic rocks initial Nd isotopic compositions relative to that of the depleted mantle model (Nelson and DePaolo 1985). Symbols show the initial isotopic composition of Nd in ten dated samples. Sample 28-1 is undated, but yields T_{DM} model age of 0.72 Ga. Note that the $\epsilon(t)$ of the Nakasib felsic rocks is approximately $\pm 1\epsilon$ unit of the model depleted mantle. **B** Comparison of crystallization age (t) and T_{DM} model age, after Harms et al. (1990). Field labeled *NE Sudan Granitoids* is from the study by Stern and Kröner (1993). Field labeled *Haya Terrane* is from the study by Kröner et al. (1991). Field labeled *Nile Craton* is generalized from the studies by Harms et al. (1990) and Stern et al. (1994). Note that Nakasib and NE Sudan samples fall close to the line $T_{DM}=t$, indicating juvenile crust without discernible contributions from older crust

diogenic growth and that of hypothetical depleted mantle (Nelson and DePaolo 1985). The ten dated samples have a narrow range of $\epsilon(t)$, between +5.5 and +7.0 (mean=+6.4). The LREE-enriched nature of all samples ($^{147}\text{Sm}/^{144}\text{Nd} = 0.116\text{--}0.149$) allows for calculation of meaningful Nd model ages for all 11 samples. There is a narrow range of T_{DM} , between 0.69 and 0.85 Ga, and the mean T_{DM} of 0.76 Ga is indistinguishable from the mean crystallization age of 0.76 Ga. Plots of the Nd data confirm the inference that the Nakasib felsic rocks are juvenile crustal additions (Fig. 5). Figure 5A compares the initial Nd isotopic composition of the ten dated samples with that expected for the depleted mantle, where it can be seen that the $\epsilon(t)$ of the Nakasib felsic rocks is approximately $\pm 1\epsilon$ unit of the model depleted mantle of Nelson and DePaolo (1985). The Nd isotopic data also indicate little or no crustal residence time for Nakasib felsic rocks, further indicating they were formed either directly by fractionation of mantle-derived melts or indirectly, by melting of mantle-derived crustal rocks. This is shown in another way in Fig. 5B, which distinguishes granitic rocks depending on whether crystallization age and Nd model ages are similar (expected for juvenile crust) or different (expected for remobilized older crust). The similarity of crystallization and Nd model ages of all Nakasib granitic rocks again demonstrates that these are juvenile additions to the crust.



Pb isotopic compositions of four K-feldspars are taken to approximate the initial Pb isotopic composition of Nakasib granitoids (Fig. 6; Table 4). These have a restricted range in $^{206}\text{Pb}/^{204}\text{Pb}$ (17.50–17.62), $^{207}\text{Pb}/^{204}\text{Pb}$ (15.45–15.58) and $^{208}\text{Pb}/^{204}\text{Pb}$ (36.95–37.15). These plot in or below the group-I or “oceanic” field of (Stacey et al. 1980), and have significantly less radiogenic $^{208}\text{Pb}/^{204}\text{Pb}$ and somewhat lower $^{206}\text{Pb}/^{204}\text{Pb}$ than the four K-feldspars

Fig. 6 Pb isotopic compositions of K-feldspars from Nakasib felsic rocks. Fields labeled *I* and *II* are oceanic and continental fields, respectively, of Stacey et al. (1980). Trend of the *Orogene* curve is from the plumbotectonics model by Zartman and Doe (1981). Field labeled *NE Sudan* is for four K-feldspars from the study by Stern and Kröner (1993). Data for galenas from the ca. 780-Ma massive sulfides of the Ariab gold district are from Wipfler (1994)

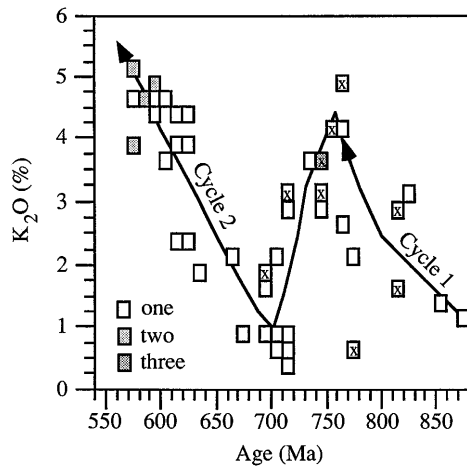


Fig. 7 Plot of K_2O vs age for plutonic igneous rocks from Sudan, Egypt, Israel, and Jordan. Data are screened to include $SiO_2 > 59\%$, error on age $\leq \pm 25$ Ma, and only samples from juvenile crustal domains (initial $^{87}Sr/^{86}Sr < 0.7035$ or region east of the Nile or Keraf suture). Data are binned into 10-million-year 0.25% K_2O intervals; means are reported for multiple analyses of individual plutons. Data sources are as follows: this study (marked with x); Bentor 1985; Beyth et al. 1994; Bielski et al. 1979; Dixon 1981a; Engel et al. 1980; Fullagar 1978; Greenberg 1981; Jarrar 1985; Jarrar et al. 1983, 1991; Katz 1996; Klemenic and Poole 1984; Kröner et al. 1990, 1991, 1994; Schandelmeier et al. 1994; Stein and Goldstein 1996; Stern and Kröner 1993; Stern and Dawoud 1991; Stern and Hedge 1985; Sturchio et al. 1984

from NE Sudan reported by Stern and Kröner (1993). The relatively homogeneous Pb isotopic compositions of the 4 K-feldspars also contrasts with the wide range found for galenas from the Ariab gold district to the west ($^{206}Pb/^{204}Pb = 17.1-17.95$; Wipfler 1994).

Discussion

These results provide new perspectives on three important aspects of crustal evolution in NE Africa during neo-Proterozoic time, including when terrane accretion began in the ANS and the significance of homogeneous and depleted mantle sources for ANS magmas. Finally, we present evidence for two cycles of LIL enrichment in ANS granitic rocks.

Beginning of terrane accretion in the ANS

Formation of the ANS involved collision of arc and other terranes during an accretion phase that culminated in collision between continental fragments of East and West Gondwanaland approximately 650 Ma (Stern 1994). The terrane accretion phase has been assigned to the interval between 630 and 715 Ma (Stoeser and Camp 1985), but our results indicate that collision between the Gebeit and Haya terranes occurred long before 715 Ma. In particular,

the Tendily granite (32-2A; 754 ± 3 Ma) is the oldest "stitching" pluton which intrudes the deformed Nakasib nappe complex and provides a minimum age for beginning of the accretion phase, at least for this region (note that plutons emplaced during late stages of deformation, such as Nakasib D₃, may still be stitching plutons). Results from other stitching plutons of similar age (740 ± 3 -Ma Luggag adamellite; 748 ± 3 -Ma Meritri granite; 762 ± 23 -Ma Wadi Agwampt granite) are consistent with the inference that collision between the Gebeit and Haya terranes occurred prior to approximately 750 Ma. This inference finds support in U-Pb zircon ages from around Bir Umq, including syntectonic tonalite (760 ± 10 Ma; Calvez and Kemp 1982) and "post-obduction" intrusions of keratophyre (764 ± 3 and 783 ± 5 Ma; Pallister et al. 1988). These data led Pallister et al. (1988) to conclude that motion on the Bir Umq thrust occurred sometime between approximately 760 Ma and approximately 840 Ma. Other Sudanese plutons of somewhat greater age (779 ± 3 -Ma Arbaat quartz diorite; 810 ± 12 -Ma Adaiamet diorite; 812 ± 18 -Ma Jebel Tala granodiorite) may not constrain the timing of collision because these are part of the Haya terrane. Because the Nakasib suture is the oldest known ANS suture (Stern and Kröner 1993; Johnson 1994), these results indicate that the accretion phase of the ANS began prior to approximately 750 Ma.

It is noteworthy that the 754-Ma Tendily body and 748-Ma Meritiri body are mapped by us as post-tectonic, whereas the 740 Ma Luggag pluton is mapped by us as syntectonic (post D₂, pre D₃). An attractive explanation is these plutons are recording the effects of heterogeneous strain, and that the development of heterogeneous strain regimes is especially appropriate for plutons emplaced in association with D₃, the waning stages of suture-related deformation.

The significance of homogeneous and depleted source characteristics

The isotopic data reported above, along with similar data from farther north in Sudan, demonstrates that the crust of this region was formed either directly (by fractionation of mantle-derived melts) or indirectly (by anatexis of mantle-derived mafic rocks) from a remarkably homogeneous and depleted mantle. Recent Nd isotopic data reported for the Eastern Desert of Egypt yield a mean $\epsilon-Nd(t)$ for 28 samples = +6.4 (Furnes et al. 1996), identical to the mean $\epsilon-Nd(t)$ obtained for the granitic rocks of the Nakasib suture. This is consistent with more extensive data showing a homogeneously nonradiogenic initial $^{87}Sr/^{86}Sr$ for eastern Egypt. The Sr and Nd isotopic data for the Eastern Desert of Egypt indicates juvenile neo-Proterozoic crust. Taken together, the isotopic data suggest that all of NE Africa north of Eritrea and Ethiopia and east of the Nile (or the Keraf suture in northern Sudan) are neo-Proterozoic additions of juvenile continental crust. There are differences in age between the intrusive rocks of this region, but they are indistinguishable in terms of initial Nd and Sr isotopic

compositions, and only slightly different in terms of feldspar Pb isotopic compositions. With few exceptions, these isotopic characteristics are shared with neo-Proterozoic igneous rocks of eastern Egypt, Sinai, Israel, Jordan, and Saudi Arabia. That the crust of this region has the isotopic signature of homogeneous, depleted mantle has been known for some time (Engel et al. 1980), and our data provide confirmation while extending these results in space and time. These data further strengthen objections to models arguing for little crustal growth during the period 800–500 Ma (Jacobsen 1988).

This isotopic homogeneity has been offered as an argument against formation of the ANS in an arc setting, and for its formation by a mantle plume (Stein and Goldstein 1996). However, the isotopic homogeneity of modern intra-oceanic arc systems is a phenomenon that is widely recognized (Morris and Hart 1983), if incompletely understood. Studies of modern arcs also show that intra-oceanic arc systems have as or more constant isotopic composition than typical hot-spot chains or flood basalt provinces. We conclude that the isotopic homogeneity documented for the neo-Proterozoic of NE Africa is not a valid argument against the arc-accretion model. All of the granitic rocks that we have analyzed have trace element compositions that are most simply explained as forming at convergent margins. Some of the 740- to 760-Ma granitic rocks plot in the field of “within-plate” granitic rocks, but this probably reflects normal processes of arc evolution and cratonization, not involvement of a mantle plume. Our data indicate that crustal evolution in the ANS during the interval 810–740 Ma was accomplished by formation of juvenile crust at intra-oceanic convergent margins, followed by collisional welding and intracrustal fractionation of arc systems to form larger tracts of increasingly differentiated continental crust.

Two enrichment cycles in the ANS?

General models for the ANS call on slow, monotonic increase in K and other LIL elements over a protracted episode of crustal growth spanning almost all of the neo-Proterozoic (Bentor 1985; Engel et al. 1980; Stoesser 1986). There are hints that this “paradigm of progressive chemical evolution” may be an oversimplification [e.g., “Early episodes of partial cratonization” of Schmidt and Brown (1984), and an important crust-formation cycle in Sinai that ended prior to 730 Ma (Kröner et al. 1990)]. Despite these suggestions, the paradigm is generally accepted.

Our chemical and geochronologic data in tandem with the results of other workers indicate that there may be two major cycles of LIL enrichment in the ANS (Fig. 7). Each cycle lasted approximately 150 million years. The first cycle began with the oldest plutonic rocks of the shield, at approximately 870 Ma. Younger plutonic rocks became progressively enriched in K – and presumably other incompatible elements – until approximately 740 Ma. This is the cycle best represented by the Nakasib plutonic rocks, and the progression for Nakasib granitic rocks seen in

Fig. 3, with early plutons falling in the low- to medium-K VAG field succeeded by 740- to 760-Ma plutons falling in the high-K VAG/WPG field, is consistent with the progressive enrichment observed for cycle-1 igneous rocks. Cycle 1 is best developed in the southern part of the ANS, in the Haya and southern Gebeit terranes of Sudan, but it is also found in the northernmost shield, in Sinai, Israel, and Jordan (Kröner et al. 1990). It is noteworthy that cycle 1 began and ended entirely within the period identified as phase II: the island arc (?) stage of Bentor (1985).

Cycle 1 ended and cycle 2 began with the emplacement of low-K tonalites to granodiorites and more mafic rocks, beginning approximately 720 Ma. This depleted suite is concentrated in the northern Gebeit terrane and SE Desert of Egypt, and includes the Serakoit Batholith of NE Sudan (Almond et al. 1984). Representatives of this suite are less abundant in the Nakasib area, although Rb–Sr mineral ages are commonly reset to an age of approximately 700 Ma (Abdelsalam 1993). These comprise a “trondhjemite–tonalite–granodiorite (TTG) suite” that corresponds to the 715- to 700-Ma episode of Stern and Hedge (1985), although granitoids of similar composition as young as 690 Ma are reported from NE Sudan (Stern and Kröner 1993), and one age of 677 ± 9 Ma was obtained for a Hafafit tonalite (EG30 of Kröner et al. 1994). For simplicity’s sake, we refer to all of these post-cycle-1 depleted granitoids as the “mid-Pan African TTG suite” and tentatively assign them to the age range of 690–720 Ma.

Valuable insights into thermal and tectonic conditions accompanying development of the mid-Pan African TTG suite can be obtained from considering the 711 ± 7 -Ma Dahanib layered komatiitic body (Dixon 1981b) and the 712 ± 24 -Ma Shadli metavolcanics (Stern et al. 1991) both in SE Egypt. The Dahanib intrusion demonstrates particularly high heat-flow conditions, because the generation of komatiitic liquids requires unusually large degrees of melting that were rarely obtained after Archean times. It should also be noted that similarly high degrees of hydrous melting at convergent margins yields boninites, whereas komatiites indicate melting of deep mantle plumes (Arndt 1994). The Shadli metavolcanics show few of the chemical hallmarks of subduction – they are not depleted in Nb and often do not plot in arc fields on trace element discrimination diagrams – and they are interpreted to have formed in a high volcanicity rift, where eruption of large volumes of compositionally bimodal lava accompanied large-scale lithospheric extension (Stern et al. 1991). Granitoids emplaced during this interval are depleted in K and LIL elements. Within the Nakasib area, the two <720-Ma samples are distinctly more depleted than the 740- to 760-Ma suite (Fig. 3), although these are not as depleted as mid-Pan African TTG bodies found farther north. High degrees of melting in an extensional setting along with a focusing of effects are features that are more consistent with development of a thermal anomaly such as a mantle plume (Stein and Goldstein 1996) than are the characteristics of older ANS rocks. Nevertheless, many of the mid-Pan African TTG suite have high Sr/Y indicating garnet control (Sr/Y as high as 70–80; Kröner et al. 1994; Stern

and Kröner 1993). Thus, these are similar to the TTG suite of Drummond and Defant (1990), and are more readily related to a subduction zone tectonic setting.

Conclusion

Granitic rocks of the Nakasib suture record magmatic evolution associated with a brief Wilson Cycle, occupying 40–50 million years from rifting at 790 Ma to the end of collisional shortening approximately 740 Ma. This study documents the oldest known example of terrane accretion in the ANS, and restricts collision to have begun sometime prior to 750 Ma. Nakasib granitic rocks preserve an early record of progressive enrichment in LIL elements that ended approximately 740 Ma. Subsequent igneous activity in the region was relatively unimportant but consisted of smaller plutons of more depleted magmas that continued until 710–696 Ma, and minor and much younger syenitic intrusions. Nakasib granitic rocks have isotopic compositions of Sr, Nd, and Pb that indicate derivation from homogeneous and depleted mantle, with no identifiable contributions from older continental crust. These data along with regional considerations indicate that an early stage of LIL enrichment in granitic magmas was interrupted approximately 720 Ma by a return to high degrees of mantle melting, possibly indicating the arrival of a mantle plume in the region.

Acknowledgements We appreciate the helpful comments and criticism of H. Schandelmeier and an anonymous referee. Our work in NE Africa was supported by NASA. Special thanks to D. Küster for making samples OSZ 13b, A8, and AW-6 available to us. This is UTD Geosciences contribution no. 868.

References

- Abdel Rahman ESM (1993) Geochemical and geotectonic controls of the metallogenic evolution of selected ophiolite complexes from the Sudan. *Berliner Geowissenschaftliche Abhandlungen A*, 145, 175 pp
- Abdelsalam MG (1993) Tectonic evolution of the Late Precambrian Nakasib suture and Oko shear zone, Red Sea Hills, Sudan. PhD dissertation, Univ Texas, Dallas
- Abdelsalam MG (1994) The Oko shear zone: post-accretionary deformation in the Arabian–Nubian shield. *J Geol Soc Lond* 151:767–776
- Abdelsalam MG, RJ Stern (1993a) Structure of the late Proterozoic Nakasib suture, Sudan. *J Geol Soc Lond* 150:1065–1074
- Abdelsalam MG, RJ Stern (1993b) Tectonic evolution of the Nakasib suture, Red Sea Hills, Sudan: evidence for a late Precambrian Wilson cycle. *J Geol Soc Lond* 150:393–404
- Abdelsalam MG, Stern RJ (1996a) Mapping Precambrian structures in the Sahara Desert with SIR-C/X-SAR radar: the Neoproterozoic Keraf suture, NE Sudan. *J Geophys Res* 101, E10: 23,063–23,076
- Abdelsalam MG, Stern RJ (1996b) Sutures and shear zones in the Arabian–Nubian shield. *J Afr Earth Sci* 23:289–310
- Almond DC, Darbyshire DPF, Ahmed F (1989) Age limit for major shearing episodes in the Nubian shield of NE Sudan. *J Afr Earth Sci* 9:489–496
- Almond DC, Ahmed F, Dawoud AS (1984) Tectonic, metamorphic, and magmatic styles in the northern Red Sea Hills of Sudan. *Bull Fac Earth Sci, King Abdulaziz U* 6:489–496
- Arndt NT (1994) Archean komatiites. In Condie KC (ed) *Archean crustal evolution*. Elsevier, Amsterdam, pp 11–44
- Bakheit AK (1991) Geochemical and tectonic control of sulphide-gold mineralization in Ariab mineral district, Red Sea Hills, Sudan. PhD dissertation, Technical Univ Berlin, 157 pp
- Beard JS (1995) Experimental, geological, and geochemical constraints on the origins of low-K silicic magmas in oceanic arcs. *J Geophys Res* 100 (15):593–600
- Bentor YK (1985) The crustal evolution of the Arabian–Nubian massif with special reference to the Sinai Peninsula. *Precambrian Res* 28:1–74
- Beyth M, Stern RJ, Altherr R, Kröner A (1994) The Late Precambrian Timna igneous complex, southern Israel: evidence for comagmatic-type sanukitoid monzodiorite and alkali granite magma. *Lithos* 31:103–124
- Bielski M, Jäger E, Steinitz G (1979) The geochronology of Iqna granite (Wadi Kid Pluton), southern Sinai. *Contrib Mineral Petrol* 70:159–165
- Calvez JY, Kemp J (1982) Geochronological investigations in the Mahd adh Dhahab quadrangle, central Arabian shield. Saudi Arabian Deputy Ministry for Mineral Resources Technical Record BRGM-TR-02-5, 41 pp
- Dixon TH, Golombek MP (1988) Late Precambrian crustal accretion rates in northeast Africa and Arabia. *Geology* 16:991–994
- Dixon TH (1981a) Age and chemical characteristics of some pre-Pan-African rocks in the Egyptian shield. *Precambrian Res* 14:119–133
- Dixon TH (1981b) Gebel Dahanib, Egypt: a Late Precambrian layered sill of komatiitic composition. *Contrib Mineral Petrol* 76:42–52
- Drummond MS, Defant MJ (1990) A model for trondhjemite–tonalite–dacite genesis and crustal growth via slab melting: Archean to modern comparisons. *J Geophys Res* 95 (21):503–521
- Dunlop HM, Kemp J, Calvez JY (1986) Geochronology and isotope geochemistry of the Bi'r Umq mafic-ultramafic complex and Arj-group volcanic rocks, Mahd adh Dhahab quadrangle, central Arabian shield. Saudi Arabian Deputy Ministry for Mineral Resources, Open-file Rep BRGM-OF-07-7, 38 pp
- Embleton JCB, Hughes DJ, Klemenic PM, Poole S, Vail J (1984) A new approach to the stratigraphy and tectonic evolution of the Red Sea Hills, Sudan. *Bull Fac Earth Sci, King Abdulaziz U* 6:113–126
- Engel AEJ, Dixon TH, Stern RJ (1980) Late Precambrian evolution of Afro-Arabian crust from ocean arc to craton. *Geol Soc Am Bull* 91:699–706
- Ewart A (1979) A review of the mineralogy and chemistry of Tertiary–Recent dacitic, latitic, rhyolitic, and related salic volcanic rocks. In: Barker F (ed) *Trondhjemites, dacites, and related rocks*. Elsevier, Amsterdam, pp 13–132
- Fullagar PD (1978) Pan-African age granites of northeastern Africa: new or reworked sialic materials? In: Salem MJ, Buswiel MT (eds) *Geology of Libya*. Academic Press, London, pp 1051–1058
- Furnes H, El-Sayed MM, Khalil SO, Hassanen MA (1996) Pan-African magmatism in the Wadi El-Imara district, Central Eastern Desert, Egypt: geochemistry and tectonic environment. *J Geol Soc Lond* 153:705–718
- Greenberg JK (1981) Characteristics and origin of Egyptian younger granites. *Geol Soc Am Bull (Part II)* 92:749–840
- Harms U, Schandelmeier H, Darbyshire DPF (1990) Pan-African reworked early/middle Proterozoic crust in NE Africa west of the Nile: Sr and Nd isotope evidence. *J Geol Soc Lond* 147:859–872
- Harris NBW, Hawkesworth CJ, Tindle AG (1993) The growth of continental crust during the Late Proterozoic: geochemical evidence from the Arabian shield. In: Prichard HM, Alabaster T, Harris NBW, Neary CR (eds) *Magmatic processes and plate tectonics*. *Geol Soc Lond Spec Publ* 76:363–371
- Henjes-Kunst F, Altherr R, Baumann A (1990) Evolution and composition of the lithospheric mantle underneath the western Arabian peninsula: constraints from Sr–Nd isotope systematics of mantle xenoliths. *Contrib Mineral Petrol* 105:460–472

- Jacobsen SB (1988) Isotopic constraints on crustal growth and recycling. *Earth Planet Sci Lett* 90:315–329
- Jarrar G (1985) Late Proterozoic crustal evolution of the Arabian–Nubian shield in the Wadi Araba area, SW Jordan. *Geol Jahrb* 61:3–87
- Jarrar G, Baumann A, Wachendorf H (1983) Age determinations in the Precambrian basement of the Wadi Araba area, southwest Jordan. *Earth Planet Sci Lett* 63:292–304
- Jarrar G, Wachendorf H, Zellmer H (1991) The Saramuj conglomerate: evolution of a Pan-African molasse sequence from southwest Jordan. *N Jahrb Geol Paläontol Mh* 6:335–356
- Johnson PR (1994) The Nakasib suture: a compilation of recent information about a Sudanese fold and thrust belt, and implications for the age, structure, and mineralization of the Bi'r Umq suture, Kingdom of Saudi Arabia. Ministry Petrol Mineral Res, Kingdom of Saudi Arabia, Open-File Rep USGS-OF-94–6, 44 pp
- Katz O (1996) The metamorphism and the structure of the South Eastern Roded Block: contribution to the Precambrian Basement evolution research. MSc thesis, Hebrew Univ, Jerusalem
- Klemenic PM, Poole S (1984) The geology and geochemistry of the Kadaweb igneous complex, Red Sea Hills, Sudan. *Bull Fac Earth Sci, King Abdulaziz U* 6:277–288
- Kröner A, Eyal M, Eyal Y (1990) Early Pan-African evolution of the basement around Elat, Israel, and the Sinai Peninsula revealed by single-zircon evaporation dating, and implications for crustal accretion rates. *Geology* 18:545–548
- Kröner A, Krüger J, Rashwan AAA (1994) Age and tectonic setting of granitoid gneisses in the Eastern Desert of Egypt and southwest Sinai. *Geol Rundsch* 83:502–513
- Kröner A, Linnebacher P, Stern RJ, Reischmann T, Manton WI, Hussein IM (1991) Evolution of Pan-African island arc assemblages in the southern Red Sea Hills, Sudan, and in southwestern Arabia as exemplified by geochemistry and geochronology. *Precambrian Res* 53:99–118
- Martin H (1986) Effect of steeper Archean geothermal gradient on geochemistry of subduction-zone magmas. *Geology* 14:753–756
- Morris JD, Hart SR (1983) Isotopic and incompatible element constraints on the genesis of island arc volcanics from Cold Bay and Amak Island, Aleutians, and implications for mantle structure. *Geochim Cosmochim Acta* 47:2015–2030
- Nassief MO, Macdonald R, Gass IG (1984) The Jebel Thurwah Upper Proterozoic ophiolite complex, western Saudi Arabia. *J Geol Soc Lond* 141:537–546
- Nelson BK, DePaolo DJ (1985) Rapid production of continental crust 1.7 to 1.9 b.y. ago: Nd isotopic evidence from the basement of the North American midcontinent. *Geol Soc Am Bull* 96:746–754
- Pallister JS, Stacey JS, Fischer LB, Premo WR (1988) Precambrian ophiolites of Arabia: geologic setting, U–Pb geochronology, Pb-isotope characteristics, and implications for continental accretion. *Precambrian Res* 38:1–54
- Pearce JA, Harris NBW, Tindle AG (1984) Trace element discrimination diagrams for the tectonic interpretation of granitic rocks. *J Petrol* 25:956–983
- Reischmann T, Kröner A (1994) Late Proterozoic island arc volcanics from Gebeit, Red Sea Hills, north-east Sudan. *Geol Rundsch* 83:547–563
- Reischmann T, Bachtadse V, Kröner A, Layer P (1992) Geochronology and palaeomagnetism of a late Proterozoic island arc terrane from the Red Sea Hills, northeast Sudan. *Earth Planet Sci Lett* 114:1–15
- Reymer A, Schubert G (1984) Phanerozoic addition rates to the continental crust and crustal growth. *Tectonics* 3:63–77
- Schandelmeier H, Abdel Rahman EM, Wipfler E, Küster D, Utke A, Matheis G (1994) Late Proterozoic magmatism in the Nakasib suture, Red Sea Hills, Sudan. *J Geol Soc Lond* 151:485–497
- Schmidt DL, Brown GF (1984) Major-element chemical evolution of the Late Proterozoic shield of Saudi Arabia. *Bull Fac Earth Sci, King Abdulaziz U* 6:2–21
- Sengör AMC, Natal'in BA (1996) Turcic-type orogeny and its role in the making of the Continental Crust. *Annu Rev Earth Planet Sci* 24:263–337
- Stacey JS, Doe BR, Roberts RJ, Delavaux MH, Gramlich JW (1980) A lead isotope study of mineralization in the Saudi Arabian shield. *Contrib Mineral Petrol* 74:175–188
- Stein M, Goldstein SL (1996) From plume head to continental lithosphere in the Arabian–Nubian shield. *Nature* 382:773–778
- Stern RJ (1994) Arc assembly and continental collision in the Neoproterozoic East African orogen: implications for the consolidation of Gondwanaland. *Annu Rev Earth Planet Sci* 22:119–151
- Stern RJ, Dawoud AS (1991) Late Precambrian (740 Ma) charnockite, enderbite, and granite from Jebel Moya, Sudan: a link between the Mozambique Belt and the Arabian–Nubian Shield? *J Geol* 99:648–659
- Stern RJ, Hedge CE (1985) Geochronologic and isotopic constraints on late Precambrian crustal evolution in the Eastern Desert of Egypt. *Am J Sci* 285:97–127
- Stern RJ, Kröner A (1993) Late Precambrian crustal evolution in NE Sudan: isotopic and geochronologic constraints. *J Geol* 101:555–574
- Stern RJ, Kröner A, Bender R, Reischmann T, Dawoud AS (1994) Precambrian basement around Wadi Halfa, Sudan: a new perspective on the evolution of the East Saharan Craton. *Geol Rundsch* 83:564–577
- Stern RJ, Kröner A, Rashwan AA (1991) A late Precambrian (~710 Ma) high volcanicity rift in the southern Eastern Desert of Egypt. *Geol Rundsch* 80:155–170
- Stoeser DB (1986) Distribution and tectonic setting of plutonic rocks of the Arabian shield. *J Afr Earth Sci* 4:21–46
- Stoeser DB, Camp VE (1985) Pan-African microplate accretion of the Arabian shield. *Geol Soc Am Bull* 96:817–826
- Sturchio N, Sultan M, Sylvester P, Batiza R, Hedge C, El Shazly EM, Abdel-Meguid A (1984) Geology, age, and origin of the Meatiq Dome: implications for the Precambrian stratigraphy and tectonic evolution of the Eastern Desert of Egypt. *Bull Fac Earth Sci, King Abdulaziz U* 6:127–143
- Vail JR (1985) Pan-African (Late Precambrian) tectonic terrains and the reconstruction of the Arabian–Nubian shield. *Geology* 13:839–842
- Weaver BL (1990) Geochemistry of highly undersaturated ocean island basalt suites from the South Atlantic Ocean: Fernando de Noronha and Trindade islands. *Contrib Mineral Petrol* 105:502–515
- Wipfler EL (1994) Geochemische, strukturelle und erzmikroskopische Untersuchungen zur Lagerstättenentwicklung des westlichen Ariab Nakasib Belt, Red Sea Provinz, NE-Sudan. *Berlin Geowiss Abh* 166:1–205
- Wipfler EL (1996) Transpressive structures in the Neoproterozoic Ariab–Nakasib Belt, northeast Sudan: evidence for suturing by oblique collision. *J Afr Earth Sci* 23:347–362
- Worku H, Schandelmeier H (1996) Tectonic evolution of the Neoproterozoic Adola Belt of southern Ethiopia: evidence for a Wilson cycle process and implications for oblique plate collision. *Precambrian Res* 77:179–210
- Zartman RE, Doe BR (1981) Plumbotectonics: the model. *Tectonophysics* 75:135–162